AIAA 79-1497R

Stability of Görtler Vortices in Boundary Layers

Jerzy M. Floryan* and William S. Saric†
Virginia Polytechnic Institute and State University, Blacksburg, Va.

A formal analysis of Görtler-type instability is presented. The boundary-layer and disturbance equations are formulated in a general, orthogonal, curvilinear system of coordinates constructed from the inviscid flow over a curved surface. Effects of curvature on the boundary-layer flow are analyzed. The basic approximation for the disturbance equations is presented and solved numerically. Previous analyses are discussed and compared with our analysis. It is shown that the general system of coordinates developed in this analysis and the correct order-of-magnitude analysis of the disturbance velocities with two velocity scales leads to a rational foundation for future work in Görtler vortices.

Nomenclature

G = $\hat{\epsilon}_c/\epsilon_v = (U_\infty \delta_r/\nu)(\delta_r/\mathcal{R})^{1/2}$, Görtler number
g = function defined in Eqs. (5) and (6)
h = $h_\phi = h_\psi$, metric coefficients for inviscid streamlines
K = $\delta_r/\mathcal{R}$, dimensionless curvature
$\mathcal{R}$ = dimensional radius of curvature of wall
R = $U_\infty \delta_r/\nu = (U_\infty x_0/\nu)^{1/2}$, Reynolds number
U, V = dimensionless basic state velocities
U_∞ = freestream velocity, reference velocity
u, v, w = dimensionless velocity components in the x, y, and z directions
x, y, z = dimensionless chordwise, normal, and spanwise coordinates
x_0 = dimensional chordwise location
$\tilde{\alpha}$ = dimensional wavenumber
α = $\tilde{\alpha}\delta_r$, dimensionless wavenumber
β = dimensionless spatial amplification rate, Eq. (23)
δ_r = $(\nu x_0/U_\infty)^{1/2}$, boundary-layer reference length
ϵ_v = $(\nu/U_\infty \delta_r)$, small viscous parameter
$\hat{\epsilon}_c$ = $(\delta_r/\mathcal{R})^{1/2}$, small curvature parameter
Λ = $(U_\infty \lambda/\nu)(\lambda/\mathcal{R})^{1/2}$, Eq. (38), dimensionless wavelength parameter
λ = $2\pi/\tilde{\alpha}$, dimensional wavelength of disturbances
ν = kinematic viscosity
ϕ = const (inviscid potential lines, chordwise coordinate)
ϕ_1 = $\epsilon_v \phi$, slow viscous scale
ϕ_2 = $\hat{\epsilon}_c \phi$, slow curvature scale
ψ = const (inviscid streamlines, normal-to-wall coordinate)

I. Introduction

DESIGNS of modern supercritical airfoils employing laminar flow control may have regions of concave curvature on the lower side of the airfoil. It is well known that a boundary layer over a concave surface has a strong inviscid instability mechanism, manifested by the presence of counter-rotating vortex pairs. The presence of streamwise vorticity is a harbinger of transition to turbulence through a coupling with Tollmien-Schlichting waves. Questions naturally arise as to the extent of the instability.

Presented as Paper 79-1497 at the AIAA 12th Fluid and Plasma Dynamics Conference, Williamsburg, Va., July 23-25, 1979; submitted Sept. 4, 1979; revision received June 30, 1981.

*Engineering Science and Mechanics Department (presently Assistant Professor, Department of Mechanical and Aerospace Engineering, Carleton University, Ottawa, Canada). Associate Member AIAA.

†Professor, Engineering Science and Mechanics Department. Associate Fellow AIAA.

While reviewing the literature one observes a plethora of analyses devoted to the stability of boundary layers over curved surfaces. Thus, we review in Sec. I.A. the different analyses of the problem that followed Görtler[1] and we discuss limitations of the previous work that resulted in many different neutral stability curves, eight of which are shown in Fig. 1. Improved calculations of the model of Smith[2] are presented and discussed in Sec. I.B. In Sec. II we develop a formally correct, first-order approximation to the complete stability equations. In Sec. II.A., we focus on the central problem in previous work: when body-oriented coordinates are used, a singularity corresponding to the center of curvature occurs in the flowfield. We introduce a general transformation to a set of orthogonal coordinates based on the streamlines and potential lines of the inviscid flowfield. The basic state is discussed in Sec. II.B. The disturbance equations are derived in Sec. II.C. with an order-of-magnitude analysis of the disturbance velocities which introduces two velocity scales. The proper boundary conditions are defined in Sec. II.C. and the solution for the disturbance equations is discussed in Sec. II.D.

In Sec. III, we describe the computational procedure. Results are given and discussed in Sec. IV.

A. Review of Previous Work

The instability of boundary layers over concave walls with perturbations in the form of streamwise vortices was first treated by Görtler.[1] The physical mechanism for such an instability is identical to that shown by Rayleigh for a rotating inviscid fluid and by Taylor for a rotating viscous fluid.[3] After Görtler, many attempts (e.g., Refs. 4-12) where made to correct, supplement, and extend his analysis. The reader is referred to Herbert[12] for a thorough review of these works. These various theoretical investigations disagreed as to the details of the formulation of the problem as well as to the fundamental properties of the instability. Figure 1 shows the collection of neutral stability curves that result from these analyses. In this figure, α is the spanwise wavenumber of the vortex pair, made dimensionless with the reference length $\delta_r = (\nu x_0/U_\infty)^{1/2}$. Here, ν is the kinematic viscosity, x_0 the chord position, and U_∞ the freestream velocity. The ordinate of Fig. 1 is the Görtler number defined as $G = R(K)^{1/2}$ where R is the Reynolds number based on δ_r and K the surface curvature normalized with δ_r. With these definitions, $R = (R_x)^{1/2}$, where R_x is the Reynolds number based in the local chord position. Herbert[12] showed that some of the disagreements between the curves in Fig. 1 are due to computational errors and he presented additional neutral curves that were not previously computed. He also showed that larger rates of decay of curvature outside the boundary layer, as well as the smaller streamwise extent of curvature, considerably

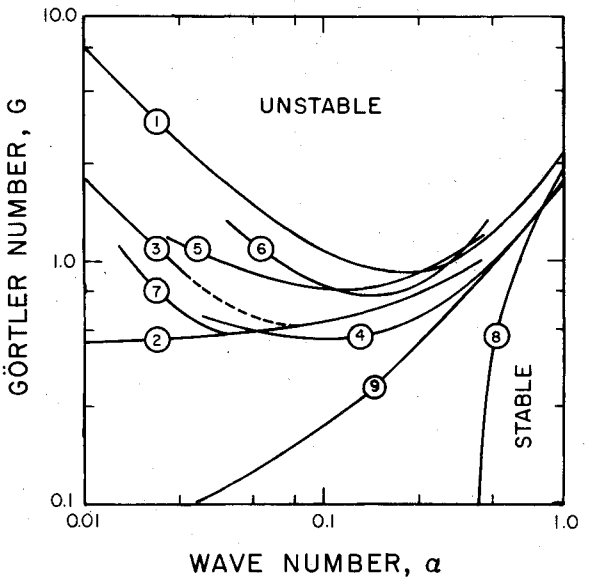

Fig. 1 Neutral curves obtained from different models of the Görtler instability (after Herbert[12]): 1) Görtler[1] model, original computations; 2) Hämmerlin[4] computations for the Görtler model; 3) Hämmerlin[5] model, includes corrections for small wavenumbers; 4) Smith[2] model, original computations; 5) Hämmerlin[6] model based on streamlines and potential lines of the flow over a wavy wall; 6) Schultz-Grunow and Behbahani[7] model; 7) Kahawita and Meroney[9,10] computations of Smith's model with the transverse velocity terms excluded; 8) Kahawita and Meroney[9,10] computations of Smith's model with the transverse velocity terms included; and 9) present calculations of Smith's model.

stabilized the flow. Another limitation of these analyses is the treatment of streamwise curvature.

Attempts to include effects of the boundary-layer growth, such as the normal-velocity terms, were made in Refs. 2, and 7-10. The problem is complicated since one has to carry a consistent approximation for the curvature terms at the same time. Smith[2] included the normal-velocity terms and was the first to include all of the second-order terms[13] from the basic state. This was followed by Kahawita and Meroney[9,10] whose equations practically match those of Smith.[2] However no arguments were presented on why the effect of curvature on the mean flow should be neglected. This problem is addressed in Sec. II of this paper.

B. Improved Calculations of Smith's Model

In addition to the problems of the treatment of the curvature, some disagreement exists between calculations of the same set of equations. Smith[2] formulated the general stability problem in terms of spatially growing disturbances and included all of the coefficients proportional to $(1-Ky)^{-n}$. He assumed $K \ll 1$ and expanded the singular terms in a power series and thus transferred the singularity to infinity. The normal-velocity terms that Smith included can be the most important nonparallel terms for boundary-layer stability when significant suction is introduced.[14]

Kahawita and Meroney[9,10] used the same equations as Smith[2] and calculated neutral curve 8 in Fig. 1. It appears that no minimum Görtler number exists. Moreover, since curve 7 has the normal-velocity terms suppressed, these terms appear to be very destabilizing whereas curve 4 given by Smith[2] differs only moderately from those obtained with the parallel-flow assumption. It has been suggested[15] that the Galerkin method used by Smith may not provide sufficient accuracy for low wavenumbers. Moreover, if one examines the eigenfunctions presented in Ref. 2, the eigenvalues computed for the high wavenumber range may correspond to the higher modes.[16] We have repeated the calculation of Smith's equations[2] for the neutral curve using a differential equation solver with orthonormalization.[17] The results of this calculation are given as curve 9 in Fig. 1 which differs from curves 4 and 8. Kahawita and Meroney[9,10] employed a routine that is almost equivalent to the procedures described in Sec. III. The shape of curve 8 appears to be due to an approximate mean flow representation and from the numerical integration itself. The detailed discussion of this and of other topics on the numerical solution are contained in Ref. 18.

II. Problem Formulation

Since the local centrifugal force drives the unstable motion, the wall curvature plays a less important role than the overall curvature of the flowfield (i.e., curvature of the streamlines). Therefore the problem is configuration dependent and may not be generalized. The most important part of this analysis is the way of approaching such problems rather than the details related to the geometrical configuration being analyzed. The model configuration considered here is general in the sense that it allows for the explicit analysis of all factors defining properties of the wall curvature, e.g., the curvature of the wall itself and its streamwise extent.

The analysis provides a formally correct, first-order approximation to the complete stability problem. The intrinsic scaling of the unstable motion is also considered by introducing two velocity scales.

A. Formulation of the Coordinate System

The influence of curvature and its streamwise extent is examined first by using the basic state as an example. Classical analyses begin with the usual system of body-oriented coordinates and are reviewed by Van Dyke.[13] When the boundary-layer-type approximation[19] is introduced into the dimensionless form of the x-momentum equation in curvilinear coordinates the following equation results

$$\frac{1}{1-Ky}U\frac{\partial U}{\partial x_1}+V\frac{\partial U}{\partial y}-\frac{K}{1-Ky}UV=-\frac{1}{1-Ky}\frac{\partial P}{\partial x_1}+\frac{\partial^2 U}{\partial y^2}-\frac{K}{1-Ky}\frac{\partial U}{\partial y}-\frac{K^2}{(1-Ky)^2}U+0\left(\frac{1}{R}\right) \tag{1}$$

where K is the dimensionless curvature, $x_1=x/R$, $1/R$ is the small dimensionless parameter characterizing the boundary-layer growth (usually $R=Re_x^{1/2}$), and $(U, V/R)$ is the basic-state velocity field. When $K \ll 1/R$, all of the curvature terms may be neglected without changing the order of the approximation and the basic state is represented by the Blasius flow. For $K=0(1/R)$, the solution of the field equations differs only slightly from the Blasius solution as far as the boundary-layer velocity profile and momentum thickness are concerned. However, the potential flow outside the boundary layer which is introduced while solving Eq. (1) is no longer a parallel flow. The coefficients of Eq. (1) tend to infinity as y approaches the center of curvature ($Ky \to 1$). The problem of this singularity in the flowfield[12] prevents a straightforward adaptation of the classical approach given by Van Dyke.[19] Thus, one has to provide a way of matching the boundary-layer flow with the potential flow so that an approximation, uniformly valid throughout the flowfield, may be produced. This may be done by introducing optimal coordinates.[20,21]

We begin by constructing a system of orthogonal coordinates that avoids singularities and has a simple representation of the boundaries. Since an analytic description of the boundary is convenient, a conformal transformation based on the Joukowski function is chosen. This transformation is capable of producing a wall with constant curvature over a certain streamwise extent. The system of coordinates constructed in this way has the straightforward physical interpretation as the set of streamlines and potential lines of the inviscid flow over a curved wall. In the wall region it has the advantages of body-oriented coordinate systems and in the

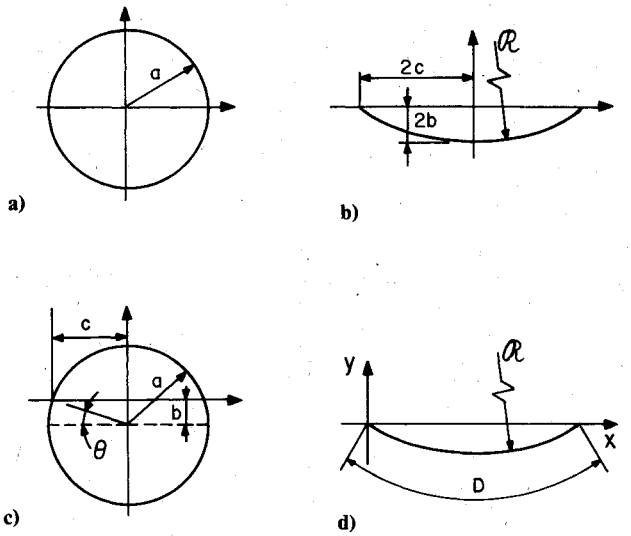

Fig. 2 The conformal transformations: a) initial configuration, E plane, $F(E)=E+a^2/E+i\,\Gamma/2\pi\ell nE-H_0$; b) step 1, S plane, $E=S+ib$; c) step 2, T plane, $T=S+c^2/S$; d) step 3, Q plane, $Q=T+2c$.

area away from the wall it assumes the form of a Cartesian system. Moreover, since this analysis is addressed to boundary-layer flows, the curvature is assumed to be small in order to use a boundary-layer-type approximation.

The sequence of transformations that produces the desired curvature is shown in Fig. 2. The initial configuration (Fig. 2a) is that of a flow around a cylinder with circulation. This is transformed into the flow over a curved wall (Fig. 2d) with the transformations shown. The circulation is fixed by application of the Kutta condition at the trailing edge. When the constant a is fixed, b/a^2 is the curvature of the wall as shown in Fig. 2b. The complex potential for Fig. 2d has the form

$$H(Q)=N+a^2/N-2b\ell n(N)-H_0 \tag{2}$$

where $N=Q/2-c+[(Q/2-c)^2-c^2]^{1/2}+ib$.

Equation (2) is an exact expression for the streamlines ψ and potential lines ϕ in terms of the reference Cartesian system, where

$$\phi=\mathrm{Re}H(Q),\ \text{potential lines}$$

$$\psi=\mathrm{Im}H(Q),\ \text{streamlines}$$

To complete this picture we require the inverse of Eq. (2) in closed form as $Q=Q(H)$. This cannot be done in general; however, one may choose the streamwise extent of the wall curvature D measured along the wall and its radius of curvature $\mathfrak{R}$ as the two parameters defining the configuration, then

$$b=\tfrac{1}{2}\mathfrak{R}\left(1-\cos\frac{D}{2\mathfrak{R}}\right)\ \text{and}\ a=\mathfrak{R}\sin\frac{D}{4\mathfrak{R}}$$

where a and b are defined in Fig. 2. When one normalizes these parameters using D as a reference scale, their dimensionless form is

$$\tilde{b}=(1/16)\epsilon_c\ \text{and}\ K=\epsilon_c$$

where $\epsilon_c=D/\mathfrak{R}$ is assumed to be a small parameter representing the magnitude of the wall curvature. Now we let $b=\epsilon_c\hat{b}$ and the transformation of Fig. 2b is assumed to be in the form

$$E=E_0+\epsilon_cE_1+\ldots \tag{3}$$

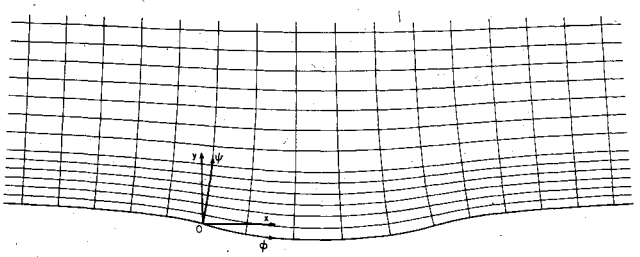

Fig. 3 System of coordinates; $0xy$ = reference Cartesian system, $0\phi\psi$ = system based on streamlines and potential lines.

Combining the transformations of Fig. 2 with Eq. (3) and collecting terms with respect to the same powers of ϵ_c we have

$$E_0=\frac{H}{2}-a+\left[\left(\frac{H}{2}-a\right)^2-a^2\right]^{1/2}$$

The Q-plane transformation (Fig. 2d) is then given as

$$Q=H+i\epsilon_c\hat{b}\left\{-2\pi i+2\ell n\left(\frac{E_0}{a}\right)-\frac{2\left[\left(\frac{H}{2}-a\right)^2-a^2\right]^{1/2}}{E_0}\right\} \tag{4}$$

where positive $\hat{b}$ corresponds to the concave curvature. The metric coefficients take the form

$$h_\phi=h_\psi=h=\left|\frac{dQ}{dH}\right|=1+\epsilon_cg(\phi,\psi) \tag{5}$$

where $g(\phi,\psi)$ can be deduced from Eq. (4).

With the boundary-layer-type analysis the expansion of the metric coefficients around $\psi=0$ is required. Therefore,

$$h_\psi=h_\phi=1+\epsilon_c\left[\frac{\hat{b}}{a^2}(4a\phi-\phi^2)^{1/2}-\frac{\hat{b}}{a^2}\psi\right]=1+\epsilon_cg \tag{6}$$

$$\frac{\partial h_\phi}{\partial\phi}=\frac{\partial h_\psi}{\partial\phi}=\epsilon_c\frac{\hat{b}}{a^2}\frac{2a-\phi}{\sqrt{4a\phi-\phi^2}} \tag{7}$$

$$\frac{\partial h_\phi}{\partial\psi}=\frac{\partial h_\psi}{\partial\psi}=-\epsilon_c\frac{\hat{b}}{a^2} \tag{8}$$

The final wall configuration is shown in Fig. 2d. The curvature of the wall, given as $\psi=0$, is computed as

$$K=\left[\frac{\partial x}{\partial\phi}\frac{\partial^2y}{\partial\phi^2}-\frac{\partial^2x}{\partial\phi^2}\frac{\partial y}{\partial\phi}\right]\Big/\left[\left(\frac{\partial x}{\partial\phi}\right)^2+\left(\frac{\partial y}{\partial\phi}\right)^2\right]^{3/2}$$

$$=\epsilon_c\frac{\hat{b}}{a^2}+0(\epsilon_c^3) \tag{9}$$

where $x=x(\phi,\psi)=\mathrm{Re}(Q)$ and $y=y(\phi,\psi)=\mathrm{Im}(Q)$. With the above relationships we are in a position to formulate and analyze the Navier-Stokes equations. Figure 3 is a typical illustration of the new coordinate system.

B. Formulation of the Basic-State Equations

The basic state is chosen to be an incompressible, constant property flow over a curved wall. Whereas the effects of curvature are represented by the small parameter ϵ_c, the effect of viscosity is represented by the small parameter ϵ_v, defined

as $\epsilon_v = (\nu/U_\infty L)^{1/2}$ where L is some reference length scale. The field equations to order ϵ_c^2 are developed by substituting the form of the metric coefficient given in Eq. (5) into the dimensionless form of the mass and momentum equations written in terms of generalized curvilinear coordinates. The results for an incompressible, two-dimensional flow are given as

Mass

$$u_\phi + v_\psi + \epsilon_c (g_\phi u + g u_\phi + g_\psi v + g v_\psi) + 0(\epsilon_c^2) = 0 \tag{10}$$

ϕ momentum

$$u_t + u u_\phi + v u_\psi + \epsilon_c (uv g_\psi + v^2 g_\phi) = -p_\phi + \epsilon_v^2 [u_{\phi\phi} + u_{\psi\psi} + \epsilon_c (-3g u_{\phi\phi} - 2g v_{\phi\psi} - g u_{\psi\psi} - 4g_\phi v_\psi + 2g_\psi v_\phi - 2g_\phi u_\phi - g_{\psi\psi} u - g_{\phi\phi} u)] + 0(\epsilon_c^2) \tag{11}$$

ψ momentum

$$v_t + u v_\phi + v v_\psi + \epsilon_c (uv g_\phi - u^2 g_\psi) = -p_\psi + \epsilon_v^2 [v_{\phi\phi} + v_{\psi\psi} + \epsilon_c (-3g v_{\psi\psi} - 2g u_{\psi\psi} - g v_{\phi\phi} + 2g_\phi u_\psi - 4g_\psi u_\phi - 2g_\psi v_\psi - g_{\phi\phi} v - g_{\psi\psi} v)] + 0(\epsilon_c^2) \tag{12}$$

where subscripts ϕ and ψ denote $\partial/\partial\phi$ and $\partial/\partial\psi$, respectively, and u and v are the velocities in the ϕ and ψ directions, respectively.

The method of matched asymptotic expansions[22] is applied to Eqs. (10-12). The solution in the outer limit $\epsilon_v \to 0$ is simple since the coordinate system is constructed in this limit. For the inner limit, we introduce the transformation $\Psi = \psi/\epsilon_v$ and assume

$$u = U_0(\phi, \Psi; \epsilon_c) + \epsilon_v U_1(\phi, \Psi; \epsilon_c) \tag{13}$$

$$v = \epsilon_v V_1(\phi, \Psi; \epsilon_c) \tag{14}$$

After the transformation and the expansion of the metric coefficients for small ψ, while retaining terms of order ϵ_c^0 and ϵ_v^0, the system of equations reduces to the familiar boundary-layer equations. That is to say, that even when ϵ_c and ϵ_v are of the same order, the boundary-layer equations over a flat plate result and the curvature effects are of a higher order. The correct zeroth-order base flow for the stability analysis is the Blasius flow. We would like to point out that the accuracy of the base flow is given as $0(\epsilon_v) + 0(\epsilon_c)$. Also, there is no problem in matching the inner and outer flow since the coordinates behave as optimal coordinates[20,21] at this level of approximation.

C. Formulation of the Disturbance Equation

The stability analysis begins with the generalized field equations expressed in the coordinate system described in Sec. II.A. The flow geometry is shown in Figs. 3 and 4. The spanwise coordinate z is a Cartesian coordinate. Three-dimensional, steady, spatially growing disturbances are superposed on the mean flow as

$$\begin{aligned} u/U_\infty &= U(\phi,\psi) + u'(\phi,\psi,z) \\ v/U_\infty &= V(\phi,\psi) + (\nu/\delta_r U_\infty) v'(\phi,\psi,z) \\ w/U_\infty &= (\nu/\delta_r U_\infty) w'(\phi,\psi,z) \\ p/\rho U_\infty^2 &= P(\phi,\psi) + (\nu^2/\delta_r^2 U_\infty^2) p'(\phi,\psi,z) \end{aligned} \tag{15}$$

In the above u, v, and w are velocity components in the ϕ, ψ, and z directions, respectively. The field equations are made dimensionless by introducing the length scale $\delta_r = (\nu x_0/U_\infty)^{1/2}$ for the ψ and z coordinates, the velocity scale U_∞ for U, V, and u', a "viscous velocity scale" ν/δ_r for v' and w', and the scale $\rho\nu^2/\delta_r^2$ for pressure disturbances. The necessity of using the different velocity scales was recognized by DiPrima and Stuart[23,24] for instabilities of this kind.

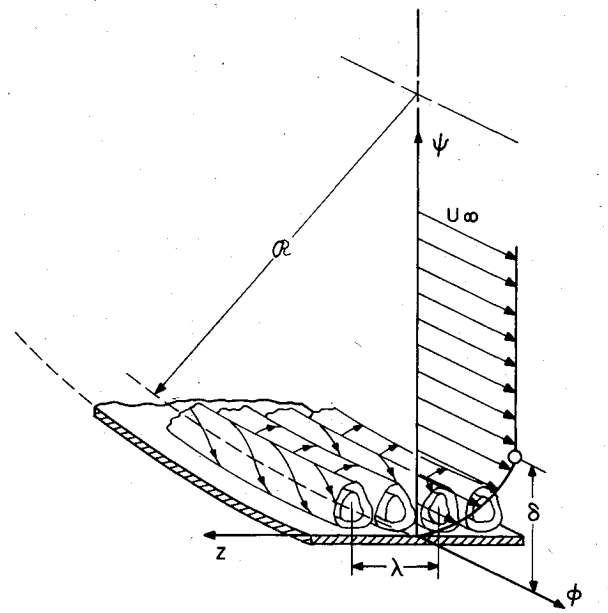

Fig. 4 Vortex-like disturbances in the boundary-layer flow over a concave wall with the axis of the vortices parallel to the principal flow direction.

The physical mechanism of the instability produces a two-dimensional motion of cellular shape in the (ψ,z) plane as shown in Fig. 4. The streamwise component of the disturbance velocity appears as a defect in the mean flow due to the vortex motion and, as such, its maximum cannot be larger than the freestream velocity.[25] Therefore it has to be scaled by the same scale as the mean flow. The different velocity scales used for v' and w' and for u' express the fact that a very weak cellular motion may produce quite large defects in the mean flow. The ratio of the two velocity scales is given by the coefficient $\epsilon_v = (\nu/\delta_r U_\infty)$ which expresses the weakness of the instability mechanism. Additional motivation for using two velocity scales may be found in the recent experiments by Bippes[26] (e.g., see his Fig. 42 on p. 164). The two different scales for disturbance velocities are crucial for this analysis. Analogously, the characteristic length for the ϕ coordinate is taken to be L and it is greater than δ_r by $1/\epsilon_v$; therefore, downstream development of disturbances is governed by the scale $\phi_1 = \epsilon_v \phi$.

Equations (15) are substituted into the field equations, the basic-state solution is applied, and the equations are linearized. Boundary-layer theory combined with the assumed scales[14] gives the chordwise variation of the mean flow in terms of the variable $\phi_1 = \epsilon_v \phi$.

The metric coefficient h was cast in terms of the streamwise extent D of the curved wall. Locally, both scales D and δ_r form a small parameter $\bar{\epsilon}_c = \delta_r/D$. It should be of the same order as ϵ_c but not equal to ϵ_c since $\bar{\epsilon}_c$ changes with the chordwise location and ϵ_c depends only upon a particular wall configuration. It is more convenient to form another parameter $\hat{\epsilon}_c = \sqrt{\epsilon_c \bar{\epsilon}_c} = \sqrt{\delta_r/\mathcal{R}}$. If δ_r, D, and $\mathcal{R}$ are known, one can formulate exact relations between ϵ_c, $\bar{\epsilon}_c$, and $\hat{\epsilon}_c$. However at this level of approximation it is enough to keep them of the same order of magnitude. The variation of the metric coefficient is governed by the scales $\phi_2 = \hat{\epsilon}_c \phi$ and $\psi_2 = \hat{\epsilon}_c \psi$ and its representation is obtained from Eqs. (6-9). The disturbance equations are formulated in terms of the new variables $(\phi_1, \phi_2, \psi, \psi_2, z)$ and the method of multiple

scales[22] is used to determine the correct asymptotic form. The zeroth-order equations are given as

Mass

$$u'_{\phi_1}+v'_{\psi}+w'_{z}=0 \tag{16}$$

ϕ momentum

$$u'U_{\phi_1}+Uu'_{\phi_1}+v'U_{\psi}+Vu'_{\psi}=u'_{\psi\psi}+u'_{zz} \tag{17}$$

ψ momentum

$$Uv'_{\phi_1}+u'V_{\phi_1}+v'V_{\psi}+Vv'_{\psi}+2G^2Uu'=-p'_{\psi}+v'_{\psi\psi}+v'_{zz} \tag{18}$$

z momentum

$$Uw'_{\phi_1}+Vw'_{\psi}=-p'_{z}+w'_{\psi\psi}+w'_{zz} \tag{19}$$

where

$$G=\hat{\epsilon}_v/\epsilon_v, \quad \text{Görtler number} \tag{20}$$

and subscripts ϕ_1, ψ, and z refer to $\partial/\partial\phi_1$, $\partial/\partial\psi$, and $\partial/\partial z$, respectively.

One should note that terms $\partial U/\partial\phi_1$, V, and $\partial V/\partial\psi$, which are of order ϵ_v, and $\partial V/\partial\phi_1$, which is of order ϵ_v^2, appear in the basic approximation for this type of instability. This suggests that the theoretical as well as experimental results may be extremely configuration dependent.

The no-slip and no-penetration boundary conditions at the wall are

$$u=v=w=0 \text{ at } \psi=0 \tag{21}$$

Away from the wall and outside the boundary layer we have

$$u=v=w\to 0 \text{ as } \psi\to\infty \tag{22}$$

which are the usual conditions for boundary-layer-type flows.

D. Normal-Mode Solution

Equations (16-19) form a set of partial differential equations of the elliptic type in (ϕ_1, ψ, z) with coefficients that depend on ϕ_1 and ψ. The dependence on z can be separated by the requirement of spanwise periodicity. The slow scale ϕ_1 may also be separated and the analysis takes on only a local meaning. The error committed is $0(\epsilon_v)$, i.e., consistent with the approximation already made. The disturbances are assumed in the form of

$$\begin{gathered}(u',v',p')=(\hat{u},\hat{v},\hat{p})\cos(\alpha z)e^{\beta\phi_1} \\ w'=\hat{w}(\psi)\sin(\alpha z)e^{\beta\phi_1}\end{gathered} \tag{23}$$

where α is the dimensionless spanwise wavenumber and β the spatial growth rate. Both α and β are assumed to be real and normalized with δ_r. Real β means that the vortices form the parallel rows that have been observed experimentally.[26,27]

Equations (23) are substituted into Eqs. (16-19), yielding

$$\beta\hat{u}+\frac{d\hat{v}}{d\psi}+\alpha\hat{w}=0 \tag{24}$$

$$\hat{u}\frac{\partial U}{\partial\phi_1}+\beta U\hat{u}+\frac{\partial U}{\partial\psi}\hat{v}+V\frac{d\hat{u}}{d\psi}=\frac{d^2\hat{u}}{d\psi^2}-\alpha^2\hat{u} \tag{25}$$

$$\begin{aligned}&\beta U\hat{v}+\frac{\partial V}{\partial\phi_1}\hat{u}+\frac{\partial V}{\partial\psi}\hat{v}+V\frac{d\hat{v}}{d\psi}+2G^2U\hat{u} \\ &=-\frac{d\hat{p}}{d\psi}+\frac{d^2\hat{v}}{d\psi^2}-\alpha^2\hat{v}\end{aligned} \tag{26}$$

$$\beta U\hat{w}+V\frac{d\hat{w}}{d\psi}=\alpha\hat{p}+\frac{d^2\hat{w}}{d\psi^2}-\alpha^2\hat{w} \tag{27}$$

The above set of equations forms a sixth-order system of homogeneous, linear, ordinary differential equations and is supplemented by the homogeneous boundary conditions of Eqs. (21) and (22). This forms an eigenvalue problem for the parameters (α, β, G). If one disregards terms due to the boundary-layer growth, Eqs. (24-27) reduce to the system presented by Görtler.[1]

III. Computational Procedure

The stability problem defined by Eqs. (21-27) is reduced to the solution of six, first-order differential equations with six homogeneous boundary conditions of the form

$$\frac{d\zeta_i}{d\psi}=M_{ij}(\psi)\zeta_j \tag{28}$$

$$\zeta_1=\zeta_3=\zeta_4=0 \text{ at } \psi=0 \tag{29}$$

$$\zeta_1=\zeta_3=\zeta_4=0 \text{ at } \psi\to\infty \tag{30}$$

$$\zeta_1=\hat{u},\ \zeta_2=\frac{d\hat{u}}{d\psi},\ \zeta_3=\hat{v},\ \zeta_4=\frac{d\hat{v}}{d\psi},\ \zeta_5=\frac{d^2\hat{v}}{d\psi^2},\ \zeta_6=\frac{d^3\hat{v}}{d\psi^3} \tag{31}$$

where M_{ij} can be easily deduced.[18] This set constitutes an eigenvalue problem and it has nontrivial solutions only for certain combinations of the parameters α, β, and G. The solution is carried out by first choosing $\psi\geq\psi_m$ such that $U=1$, $\partial U/\partial\psi=0$, $\partial U/\partial\phi_1=0$, $\partial^2U/\partial\phi_1\partial\psi=0$, $V=\text{const}$, $\partial V/\partial\psi=0$, and $\partial V/\partial\phi_1=\text{const}$. Then, for $\psi\geq\psi_m$, Eq. (28) reduces to an equation with constant coefficients whose linearly independent solutions have the form

$$\zeta_i=\Lambda_{ik}\exp(\lambda_k\psi) \qquad i,k=1,\ldots,6 \tag{32}$$

where λ_k are the eigenvalues of the matrix $M_{ij}\mid_{\psi>\psi_m}$ given by

$$\begin{aligned}\lambda_{1,2}&=\pm\alpha \\ \lambda_{3,4}&=\tfrac{1}{2}\left[V\pm\sqrt{V^2+4(\beta+\alpha^2)}\right] \\ \lambda_{5,6}&=\lambda_{3,4}\end{aligned} \tag{33}$$

and Λ_{ik} is the eigenvector matrix. Because of the repeated eigenvalues, proper care has to be taken for their respective eigenvectors. The boundary conditions applied at $\psi\to\infty$ are satisfied by eliminating solutions characterized by positive eigenvalues in Eq. (33). Then a linear combination of the remaining solutions is used as a starting condition at $\psi=\psi_m$ and the forward integration routine[17] is used to find the eigenfunctions and eigenvalues. Given α, β, and a guess for G, a fifth-order, variable step-size algorithm coupled with orthonormalization[17] is used to integrate Eq. (28) from $\psi=\psi_m$ to $\psi=0$. A linear combination of solutions is found to satisfy the conditions $\zeta_1(0)=\zeta_3(0)=0$. If an eigenvalue G has been used, the third condition $\zeta_4(0)=0$ is satisfied; otherwise, G is incremented by using a Newton-Raphson procedure and the procedure is repeated until $\zeta_4(0)=0$.

For the test purposes, the system *adjoint* to Eq. (28) is formed by the differential equations[18]

$$d\zeta_i^*/d\psi=-M_{ij}^*\zeta_j^* \tag{34}$$

with homogeneous boundary conditions on ζ_2^*, ζ_5^*, ζ_6^*, and M_{ij}^* the transpose of the complex conjugate of M_{ij}. The com-

putations were carried until eigenvalues calculated from the system defined by Eq. (28) and its adjoint [Eq. (34)] independently agreed and were independent of the accuracy of the integrator. The use of the adjoint system is a very reliable and easy to use method for verification of the eigenvalues. It was also necessary to check the shape of the eigenfunctions in order to differentiate between the basic and higher modes. This was especially important when $\alpha = 0(1)$ or higher.

IV. Results and Discussion

Smith's equations have been solved again during the present study as discussed in Sec. I.B. The results for the neutral stability case are presented as curve 2 in Fig. 5. Curve 3 in Fig. 5 is the result of the present study which was obtained from the solution of Eqs. (28-31). As it is seen, Smith's model overestimates the instability, especially in the small wavenumber region. The results of the computations with the present model that were reported earlier in the preprint of this paper were affected by the improper representation of the term $\partial V/\partial\phi_1$ in the calculation of the mean flow. This resulted in its absence outside the boundary layer as was pointed out by Ragab and Nayfeh.[28] (The neutral curves in the original paper are wrong and have been corrected here.) Thus curve 3 in Fig. 5 is identical to that found by Ragab and Nayfeh.[28]

Curves of constant growth rate computed with the equations given in Sec. III were compared with those calculated by Smith[2] for the Blasius boundary layer. The agreement in the region of wavenumbers of practical interest is moderate. In the small wavenumber region differences of as much as 60-100% may occur between the two models.[18] These differences will accumulate when integrated for the total growth. There is also some difference in the loci of maximum amplification rates. A more precise statement about the differences between the curves of constant amplification rate cannot be made since computations of these curves based on Smith's equations do not yield a solution of practical value for $\beta \neq 0$ and it was decided not to introduce any additional simplifications.[18]

A. Discussion of the Present Model

The final formulation of the present model is given by Eqs. (16-20). This model is a formally correct, basic approximation to the field equations describing the stability of boundary layers over curved walls with respect to Görtler vortices. The correct mean flow is given by the basic boundary-layer equations. The disturbance equations are obtained by the limits of $\hat{\epsilon}_c \to 0$ and $\epsilon_v \to 0$ with $G = \hat{\epsilon}_c/\epsilon_v$ fixed.

An additional length scale due to the streamwise extent of the curved wall, the variation of the streamline curvature away from the wall, displacement thickness effects, and the use of the viscous streamlines as coordinates are all features of the second-order theory.

The physical instability mechanism produces a vortex motion in the (ψ,z) plane as shown in Fig. 4. This phenomenon is very weak and difficult to observe. It modifies the basic flow by convecting particles away and toward the wall, preserving their original basic-state velocities. In the interpretation presented here, the streamwise disturbance velocity component represents the defect in the basic flow, which is only indirectly produced by the instability. Thus, the u component cannot be larger than the maximum of the streamwise velocity component of the basic flow which has been proved by Kirchgässner.[25] Since the streamwise disturbance velocity component constitutes a fraction of the basic flow, it is of the same order of magnitude as the basic flow itself. The disturbance velocity components forming the vortex motion are produced directly by the weak instability and therefore appear to be of an order of magnitude smaller than the streamwise component. The transport of momentum due to the disturbance motion follows a similar ordering. Examine the left-hand side of Eq. (17) and recall from Sec. II that the velocity components are assigned the following ordering: $U = 0(1)$, $V = 0(\epsilon_v)$, $u' = 0(1)$, $v' = 0(\epsilon_v)$, and $w' = 0(\epsilon_v)$. Derivatives with respect to ψ and z are $0(1)$ while derivatives with respect to ϕ_1 are $0(\epsilon_v)$. Then, it is straightforward to show that Eq. (17) describes $0(\epsilon_v)$ transport of momentum that is of the same order of magnitude as the boundary-layer streamwise momentum transport. Thus, the streamwise modulation of the basic flow brings $0(1)$ contributions to the streamwise disturbance momentum transport. Equations (18) and (19) describe transport of momentum that is $0(\epsilon_v^2)$. Thus, the basic-state terms, that are $0(\epsilon_v^2)$ according to boundary-layer theory, bring $0(1)$ contributions to the normal-to-the-wall disturbance momentum transport. The difference in the scaling of the disturbance momentum transport equations is consistent with the interpretation of a weak instability, vortex-type motion that indirectly produces a large defect in the basic flow. However, the indirect effect of the unstable motion, the u component, is the easiest to identify and to measure.

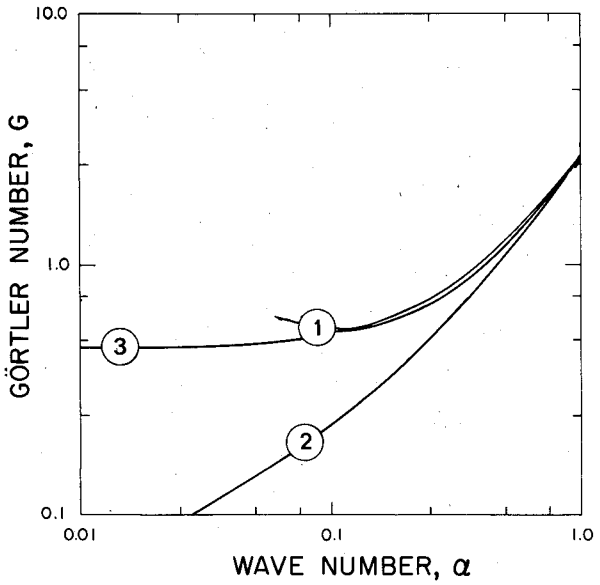

Fig. 5 Comparisons of different computations of the neutral stability curve based on the present model and that of Smith[2]: 1) Smith's[2] original computations; 2) present computations with Smith's model; 3) present model.

B. Critical Stability Conditions and Small-Wavenumber Limit

The computations of the neutral curve 3 in Fig. 5 were carried out to wavenumbers of $\alpha = 10^{-6}$ and neutral curve appears to asymptotically level off at $G = 0.4638$. There is no change in the last digit from $\alpha = 10^{-4}$ to 10^{-6}; therefore this value of Görtler number may be considered as a critical value for the Blasius boundary layer.

Additional information about the behavior of the stability characteristics for the low wavenumber limit (always taken as $\alpha \to 0^+$) are obtained from the expression of $dG/d\alpha$. Three cases for the curves of constant amplification rates are possible, i.e.,

$$1) \quad \lim_{\alpha \to 0} \frac{dG}{d\alpha} = C_1 > 0$$

$$2) \quad \lim_{\alpha \to 0} \frac{dG}{d\alpha} = 0$$

$$3) \quad \lim_{\alpha \to 0} \frac{dG}{d\alpha} = C_2 < 0$$

where C_1 and C_2 are constants.

Thus, in case 1 the curve may reach a certain limiting, finite value of the Görtler number at $\alpha=0$. In case 2 this value is reached asymptotically as $\alpha\to 0$ and therefore, it may be determined for a certain finite wavenumber $\alpha>0$. In case 3 the curve possesses a minimum at a certain wavenumber $\alpha\neq 0$.

The expression $dG/d\alpha$ is evaluated with the help of Eqs. (28). Since only the curves of constant amplification rates are considered, $d\beta/d\alpha$ is taken to be zero. Differentiation of Eqs. (28) with respect to α^2 gives

$$d\zeta_i'/d\psi = M_{ij}(\psi)\zeta_i' + M_{ij}'(\psi)\zeta_i \tag{35}$$

where

$$\zeta_i' = d\zeta_i/d(\alpha^2) \quad \text{and} \quad M_{ij}' = dM_{ij}/d(\alpha^2)$$

Equations (35), when supplemented by boundary conditions (29) and (30), form an inhomogeneous boundary-value problem. Since the homogeneous part of Eqs. (35) is the same as Eqs. (28) and since the latter have a nontrivial solution, Eqs. (35) have a solution if, and only if, the inhomogeneous parts are orthogonal to every solution of the adjoint homogeneous problem. Then

$$\frac{dG}{d\alpha} = \left\{\int_0^\infty \left[\zeta_1\zeta_2^* - \left(\frac{\partial U}{\partial \phi_1} + 2G^2U\right)\zeta_1\zeta_6^* - \left(\beta U + \frac{\partial V}{\partial \psi} - \alpha^2\right) \times \zeta_3\zeta_6^* - V\zeta_4\zeta_6^* + 2\zeta_5\zeta_6^*\right] d\psi\right\} \Big/ 2G\alpha\int_0^\infty U\zeta_1\zeta_6^* d\psi \tag{36}$$

where ζ_i and ζ_i^* are solutions of Eqs. (28) and (34), respectively. When amplified disturbances are considered, curves of constant amplification rate in the plane $(\ell nG, \ell n\alpha)$ form straight lines with a negative tangent in the limit of $\alpha\to 0$ (Fig. 6). Thus

$$\frac{dG}{d\alpha} = \frac{G}{\alpha}\frac{d(\ell nG)}{d(\ell n\alpha)} = \frac{G}{\alpha}C \tag{37}$$

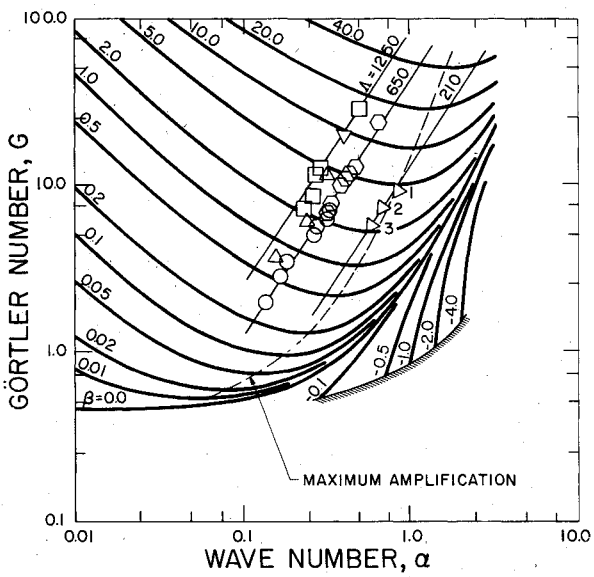

Fig. 6 Curves of constant amplification rate as a function of Görtler number, $G=U_\infty\delta_r/\nu\sqrt{\delta_r/\Re}$, and wavenumber α for the Blasius boundary layer: comparison of theory with experiments. The shaded line corresponds to a combination of eigenvalues in Eq. (33) that does not permit satisfying the homogeneous boundary conditions as $\psi\to\infty$. Experimental points due to Tani and Sakagami[30]: ○ $U_\infty=11$ m/s, $\Re=10$ m; □ $U_\infty=7$ m/s, $\Re=5$ m; ⬡ $U_\infty=7$ m/s, $\Re=3$ m; △ $U_\infty=16$ m/s, $\Re=10$ m; ▽ $U_\infty=7$ m/s, $\Re=1$ m. Experimental points due to Bippes[26]: ▷1 $U_\infty=0.3$ m/s, $\Re=0.5$ m; ▷2 $U_\infty=0.075$ m/s, $\Re=0.5$ m; ▷3 $U_\infty=0.075$ m/s, $\Re=1.0$ m.

where C is a constant. However, G becomes large as $\alpha\to 0$, according to extended calculations[18] of Fig. 6 with $\beta\neq 0$. If one examines Eq. (36), the dominant term in the numerator in the limit $\alpha\to 0$, is $2G^2U\zeta_1\zeta_6^*$. Thus, Eq. (36) reduces to the form of Eq. (37) with $C=-1$ in agreement with Fig. 6. It is difficult to make a priori predictions about the behavior of the curves of constant amplification rate in the limit as $\alpha\to 0$ based only on the examination of Eq. (36). The exact predictions require numerical evaluation of Eq. (37) and this is no more advantageous than the direct numerical integration of Eqs. (28).

C. Comparison with Experiments

The experimental points due to Tani,[29] Tani and Sakagami,[30] and Bippes[26] are plotted in Fig. 6 and are located in the region where the disturbances are to be amplified according to the theory. However, the theory predicts nothing about which wavenumber will actually appear for a given radius of curvature and flow conditions. The apparent indifference of the flow to the wavenumber is supported by the experimental findings. The wavelength of the vortices is determined by the particular edge effects of the experimental apparatus (Tani and Sakagami[30]) or by the oncoming disturbances (Bippes[26]). These observations should not be surprising since the instability mechanism is weak. Any external factor imposed on the flow after the instability mechanism is activated and before the effects of its action are observable may give rise to almost any wavenumber. Bippes[26] conducted experiments with screens in order to produce an isotropic field of disturbances in the oncoming flow. Then, out of the entire variety of disturbance components in the oncoming flow, only those corresponding to a longitudinal vortex component of a certain wavelength were excited. This wavelength corresponded to the maximum amplification rate predicted by the linear theory (Fig. 6).

In all experimental observations, it was noted that the dimensional wavelength (or wavenumber) of the disturbance was conserved in the flow direction. Since the dimensionless wavenumber α is normalized with δ_r, it is a variable in the flow direction. It is convenient, therefore, to introduce a dimensionless wavelength parameter Λ which is constant in the flow direction. Thus we follow Bippes[26] and define

$$\Lambda = (U_\infty\lambda/\nu)(\lambda/\Re)^{1/2} \tag{38}$$

where λ is the dimensional wavelength in the z direction.‡ In the stability diagram of Fig. 6, the lines of Λ equal a constant, are straight with tangent 3/2. For some range of parameters (G, α) the line of maximum amplification is parallel to the line Λ equal a constant, which suggests that a wavenumber corresponding to this particular value of Λ has the optimal conditions to grow. This idea may be better followed in Fig. 7, which is a stability diagram in the (G, Λ) plane. Note that for the fixed curvature and flow conditions, the (G, Λ) plane may be interpreted as the $(\delta_r^{3/2}, \lambda^{3/2})$ plane. Otherwise Λ plays the role of a Görtler number based on a different length scale, say G_λ.

The experimental verification of the location of the neutral curve is due to Wortmann,[31,32] and Bippes.[26] Wortmann's neutral point is located above the neutral curve shown in Fig. 8. Bippes limited himself to the right part of the neutral curve only, where $\alpha=0(1)$ and the neutral curve is not strongly influenced by the effect of the boundary-layer growth. The experimentally located neutral curve is moved toward larger wavenumbers as compared to its theoretical counterpart.

‡One can similarly define a wavenumber parameter $A=(\alpha\nu/U_\infty)(\alpha\Re)^{1/2}$, which would play the same role as Λ given by Eq. (38). Both A and Λ would remain constant in the flow direction. These parameters are analogous to the frequency parameter, $F=2\pi f\nu/U_\infty^2$, used in the presentation of the experimental data of Tollmien-Schlichting waves.

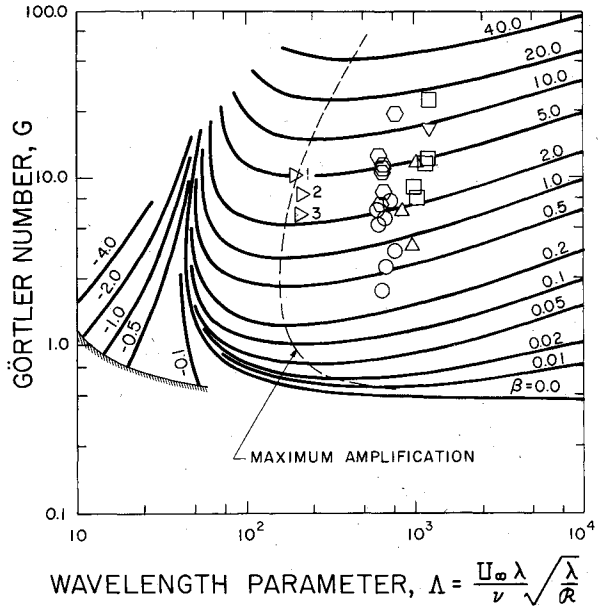

Fig. 7 Curves of constant amplification rate as a function of Görtler number, $G = U_\infty \delta_r / \nu\sqrt{\delta_r/\mathcal{R}}$, and the wavelength parameter, $\Lambda = U_\infty \lambda / \nu\sqrt{\lambda/\mathcal{R}}$, for the Blasius boundary layer (same notation as Fig. 6).

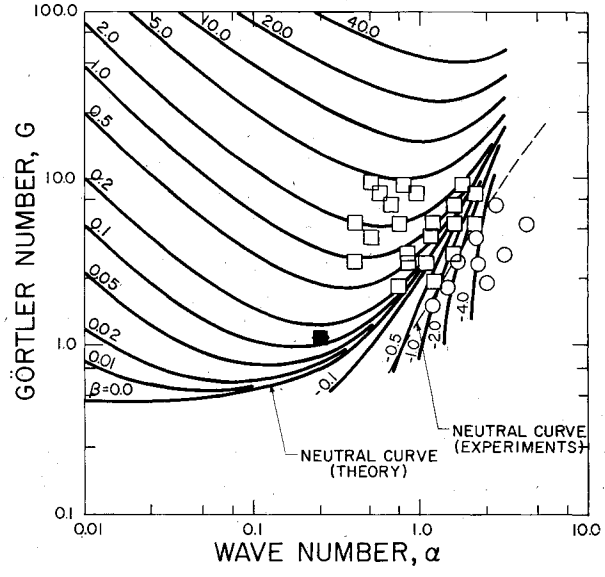

Fig. 8 Location of the neutral curve for the Blasius boundary layer: comparison of theory with experiments. Experimental points due to Bippes[26]: o attenuated disturbances, □ amplified disturbances; experimental points due to Wortmann[31,32]: ■ neutral disturbances.

Bippes[26] suggests that the damping rates are small, concluding that it is impossible to locate the neutral curve precisely. This lack of precision may account for the difference in the location of the neutral curves. However, according to the calculations shown in Fig. 8, it appears that the magnitudes of the growth and decay rates are comparable on both sides of the neutral curve. The reasons accounting for the difference in the location of the neutral curve are not well understood as yet.

D. The Cutoff Wavelength and Attenuation

The form of the neutral curve given in Fig. 7 defines the range of the disturbance wavelengths that are never amplified, according to the linear theory. The cutoff wavelength parameter, defining the upper bound for the disturbance wavelength that is always attenuated, takes the value $\Lambda_c = 44.29$ for the Blasius boundary layer.

Curves of constant damping rates are given in Figs. 6 and 7. The region of small Görtler numbers and large wavenumbers is characterized by the existence of the complex eigenvalues in the asymptotic solution outside the boundary layer, given by Eq. (33). Therefore, for large damping rates, a single vortex may split into a set of vortices located one over another.

For certain values of damping rates, the eigenvalues given by Eq. (33) prohibit satisfying the outer boundary conditions as $\psi \to \infty$. These conditions are uniquely satisfied if Eq. (33) possesses three positive and three negative eigenvalues. When the number of positive eigenvalues is larger than three, the outer boundary conditions cannot be satisfied. The Görtler numbers and wavenumbers corresponding to the unfavorable change in the configuration of eigenvalues are shown in Figs. 6 and 7. It should be noted that complex eigenvalues appear for Görtler numbers smaller than those corresponding to the first occurrence of the unfavorable configuration of eigenvalues, as described above. The above-described problems raise the question of whether the highly damped disturbances exist in the assumed form of Eq. (33) or whether certain types of oscillatory solutions must be admitted, say in the form of a traveling wave in the chordwise direction.

Acknowledgment

This work was supported by NASA Langley Research Center under Grant NSG-1255.

References

[1] Görtler, H., "Instabilität laminarer Grenzchichten an konkaven Wänden gegenüber gewissen dreidimensionalen Störungen," *ZAMM,* Vol. 21, No. 1, 1941, pp. 250-252 (also NACA-TM-1375, 1954).

[2] Smith, A. M. O., "On the Growth of Taylor-Görtler Vortices Along Highly Concave Walls," *Quarterly Journal of Applied Mathematics,* Vol. 13, No. 3, 1955, pp. 233-262 (also Douglas Aircraft Rept. ES-17110, 1953).

[3] Chandrasekhar, S., *Hydrodynamic and Hydromagnetic Stability,* Oxford Press, Oxford, England, 1961.

[4] Hammerlin, G., "Über die dreidimensionale Instabilität laminar Grenzschichten," *ZAMM,* Vol. 35, Sept. 1955, pp. 366-367.

[5] Hämmerlin, G., "Über das Eigenwertproblem der dreidimensionalen Instabilität laminarer Grenzchichten an konkaven Wänden," *Journal Rational Mechanics and Analysis,* Vol. 4, No. 2, 1955, pp. 279-321.

[6] Hämmerlin, G., "Über die Stabilität einer kompressiblen Strömung längs einer konkaven Wand bei verschiedenen Wandtemperaturverhältnissen," *Deutsche Versuchsanstalt für Luftfahrt,* Bericht 176, 1961.

[7] Schultz-Grunow, F. and Behbahani, D., "Boundary Layer Stability on Longitudinally Curved Walls," *ZAMP,* Vol. 24, No. 4, 1973, pp. 499-506.

[8] Behbahani, D., "Stability of Laminar Boundary Layers along Longitudinally Curved Walls," *ZAMP,* Vol. 26, No. 4, 1975, pp. 493-495.

[9] Kahawita, R. A. and Meroney, R. N., "The Stability of Parallel, Quasi-Parallel and Stationary Flows," Project Themis TR24, Colorado State University, Fort Collins, Colo., Sept. 1973.

[10] Kahawita, R. A. and Meroney, R. N., "The Influence of Heating on the Stability of Laminar Boundary Layers along Concave Curved Walls," *Transactions of ASME, Journal of Applied Mechanics,* Vol. 44, March 1977, pp. 11-17.

[11] Tobak, M., "On Local Görtler Instability," *ZAMP,* Vol. 22, No. 1, 1971, pp. 130-143.

[12] Herbert, Th., "On the Stability of the Boundary Layer along a Concave Wall," *Archiwum Mechaniki Stosowanej,* Vol. 28, No. 5-6, 1976, pp. 1039-1055.

[13] Van Dyke, M., "Higher-Order Boundary Layer Theory," *Annual Review of Fluid Mechanics,* Vol. 1, 1964, pp. 265-292.

[14] Saric, W. S. and Nayfeh, A. H., "Nonparallel Stability of Boundary Layer Flows with Pressure Gradients and Suction," *AGARD Symposium Laminar-Turbulent Transition,* AGARD Proceedings 224, May 1977, Paper 6, pp. 6.1-6.23

[15] Chang, T. S. and Sartory, W. K., "Hydromagnetic Görtler Instability in a Boundary Layer on a Concave Wall," *Developments in Theoretical and Applied Mechanics,* Vol. 4, Academic Press, New York, 1964, pp. 489-500.

[16] Herbert, Th., "Higher Eigenstates of Görtler Vortices," *Theoretical and Experimental Fluid Mechanics,* edited by U. Müller, K. B. Roesner, and B. Schmidt, Springer-Verlag, New York, 1979, pp. 322-330.

[17] Scott, R. R. and Watts, H. A., "Computational Solution of Linear Two-Point Boundary-Value Problems via Orthonormalization," *SIAM Journal of Numerical Analysis,* Vol. 14, No. 1, 1977, pp. 40-70.

[18] Floryan, J. M., "Stability of Boundary-Layer Flows over Curved Walls," Ph.D. Thesis, Virginia Polytechnic Institute and State University, Blacksburg, Va., Jan. 1980.

[19] Van Dyke, M., "Higher Approximations in Boundary-Layer Theory, Pt. 1: General Analysis, Pt. 2: Application to Leading Edges," *Journal of Fluid Mechanics,* Vol. 14, 1962, Part 2 pp. 161-177 and Part 4, pp. 481-495.

[20] Davis, R. T., "A Study of the Use of Optimal Coordinates in the Solution of the Navier-Stokes Equations," Dept. of Aerospace Engineering, University of Cincinnati, Rept. AFL-74-12-14, 1974.

[21] Crespo da Silva, M. R. M. and Davis, R. T., "A Study of Optimal Coordinate Theory with Application to Several Physical Problems," *International Journal of Engineering Science,* Vol. 15, No. 7, 1977, pp. 455-464.

[22] Nayfeh, A. H., *Perturbations Methods,* Wiley-Interscience, New York, 1973.

[23] DiPrima, R. C. and Stuart, J. T., "Non-Local Effects in the Stability of Flow between Eccentric Rotating Cylinders," *Journal of Fluid Mechanics,* Vol. 54, Part 3, 1972, pp. 393-415.

[24] DiPrima, R. C. and Stuart, J. T., "The Nonlinear Calculation of Taylor Vortex Flow between Eccentric Rotating Cylinders," *Journal of Fluid Mechanics,* Vol. 67, Part 1, 1975, pp. 85-111.

[25] Kirchgässner, K., "Beiträge zu einer nichtlineraren theorie der stabilität von schichtenströmungen längs zylindrisch gekrümmter wände gegenüber dreidimensionalen störungen," *Archive Rational Mechanics and Analysis,* Vol. 6, No. 1, 1960, pp. 20-33.

[26] Bippes, H., "Experimentelle Untersuchung des laminar-turbulenten Umschlags an einer parallel angeströmten konkaven Wand," Sitzungsberichte der Heidelberger Akademie der Wissenschaften Mathematischnaturwissenschaftliche Klasse, 3 Abhandlund, Jahrgang 1972, pp. 103-180 (also NASA-TM-72243, March 1978).

[27] Bippes, H. and Görtler, H., "Dreidimensionale störungen in der Grenzschicht an einer könkaven wand," *Acta Mechanica,* Vol. 14, No. 4, 1972, pp. 251-267.

[28] Ragab, S. A. and Nayfeh, A. H., "Effect of Pressure Gradients on Görtler Instability," AIAA Paper 80-1377, July 1980.

[29] Tani, I., "Production of Longitudinal Vortices in the Boundary Layer along a Curved Wall," *Journal of Geophysical Research,* Vol. 67, No. 8, 1962, pp. 3075-3080.

[30] Tani, I. and Sakagami, J., "Boundary Layer Instability at Subsonic Speeds," *Proceedings of Third Congress of International Council of Aerospace Sciences,* Stockholm, 1962, Spartan, Washington, D. C., 1964, pp. 391-403.

[31] Wortmann, F. X., "Experimentelle Untersuchungen laminarer Grenzschichten bei instabilier Schichtung," *Proceedings of XI International Congress on Applied Mechanics,* Munich, edited by H. Görtler, Springer-Verlag, Berlin, 1964, pp. 815-825.

[32] Wortmann, F. X., "Experimental Investigations of Vortex Occurrence at Transition in Unstable Laminar Boundary Layers," AFOSR Rept. 64-1280, AF 61 (052)-220, 1964.